Remote Sensing Applications: Society and Environment 41 (2026) 101836

Contents lists available at ScienceDirect

Remote Sensing Applications: Society and Environment

journal homepage: www.elsevier.com/locate/rsase

# An automated Google Earth Engine application for detecting the impacted area of treeless boreal peatland restoration – A tool for practitioners and decision-makers

Aleksi Isoaho [a,*], Timo P. Pitkänen [b], Lauri Ikkala [c], Antti Sallinen [d], Parvez Rana [b], Hannu Marttila [e], Lassi Päkkilä [e], Aleksi Räsänen [f]

[a] Natural Resources Institute Finland (Luke), Paavo Havaksen tie 3, FI-90570 Oulu, Finland
[b] Natural Resources Institute Finland (Luke), Latokartanonkaari 9, FI-00790 Helsinki, Finland
[c] Geological Survey of Finland (GTK), Teknologiakatu 7, Kokkola, FI-67101, Finland
[d] Finnish Environment Institute (Syke), Yliopistokatu 6 B, FI-80100 Joensuu, Finland
[e] Water, Energy and Environmental Engineering Research Unit, Faculty of Technology, University of Oulu, P.O. Box 4300, Oulu, Finland
[f] Geography Research Unit, Faculty of Science, University of Oulu, P.O. Box 8000, Oulu, Finland

ARTICLE INFO

*Keywords:*
Remote sensing
Change detection
Sentinel-2
Landsat
Peatland
Hydrology
Monitoring

ABSTRACT

Remote sensing (RS) methods are recognized as a potential solution for the increasing need to monitor peatland changes after restoration, but practical monitoring tools are lacking. To address this gap, our objective is to (1) test which optical satellite variables can be used for detecting hydrological restoration impact in treeless boreal peatlands, (2) develop a user-friendly Google Earth Engine (GEE) application based on the results, and (3) demonstrate its usage in practice. Firstly, by utilizing data from 24 peatland restoration sites in Finland, we used Mann-Whitney *U* test and Kruskal-Wallis test to determine which optical variables calculated from Sentinel-2 and Landsat 8–9 satellite imagery can be used as indicators for surface wetness changes after peatland restoration. The results from statistical tests indicated that near-infrared (NIR) and shortwave infrared (SWIR) bands were the most effective in detecting the impact. Secondly, we incorporated the NIR and SWIR bands into the GEE application to indicate the location and magnitude of restoration impact. The developed application uses a direct input from the openly available satellite imagery archives and requires only a few inputs from the user for the case-specific analysis, making it user-friendly. The application calculates cloudless and representative satellite image mosaics and uses change detection for the situations before and after restoration to show the hydrological restoration impacts spatially. The application provides researchers, stakeholders, decision-makers, and practitioners with limited technical experience the possibility to use satellite imagery for assessing restoration impacts in open or sparsely treed peatlands in boreal landscapes.

## 1. Introduction

Peatlands support unique biodiversity and are important carbon storages and provide several other ecosystem services (Yu et al.,

* Corresponding author.
*E-mail address:* aleksi.isoaho@luke.fi (A. Isoaho).

https://doi.org/10.1016/j.rsase.2025.101836
Received 12 March 2025; Received in revised form 14 November 2025; Accepted 11 December 2025
Available online 13 December 2025
2352-9385/© 2025 The Authors. Published by Elsevier B.V. This is an open access article under the CC BY license (http://creativecommons.org/licenses/by/4.0/).

2010; Ramchunder et al., 2012; Bonn et al., 2016; Harris et al., 2022). However, human influence has caused peatlands to deteriorate globally (Leifeld and Menichetti, 2018). Ecological restoration of peatlands has emerged as a strategy to safeguard biodiversity and ecosystem functioning (Suding, 2011), to reverse degradation, and to recover the peatland ecosystems towards a pristine state (Gann et al., 2019).

Peatland restoration activities are projected to increase; for example, in the European Union, the Nature Restoration Law aims to restore 90 % of ecosystems in poor condition by 2050 (Regulation (EU) 2024/1991). Based on initial estimates, in Finland alone, up to 2.6 million ha of peatlands may need to be restored (Räsänen et al., 2023). The law also states that restoration measures need to be monitored and validated. Therefore, new cost-efficient monitoring methods are needed so that stakeholders and practitioners can evaluate the effectiveness of the restoration efforts.

In northern Europe, especially in Finland, forestry drainage has been a major factor contributing to the peatland degradation (Vasander et al., 2003; Minkkinen et al., 2008). Forestry drainage lowers the water table, which in turn initiates a shift in plant communities towards drier forest vegetation (Laine et al., 2006; Maanavilja et al., 2014). The drainage also has catchment-level effects as it changes the water flow routes (Holden et al., 2006; Menberu et al., 2018; Sallinen et al., 2019). This causes major ecohydrological changes, particularly in minerotrophic peatland complexes known as aapa mires, in which vegetation patterns rely heavily on snowmelt input and runoff from the catchment area upstream (Sallinen et al., 2019, 2023). Recent studies in several aapa mires indicate that the wet central areas consisting of flark fens are changing towards drier bog-like vegetation, probably as a result of decreased surface-water input and climate change (Tahvanainen, 2011; Kolari et al., 2022; Granlund et al., 2022; Heikkinen et al., 2023).

Restoration of forestry-drained peatlands is typically conducted by measures primarily aiming at recovering the hydrology, such as infilling and damming the drainage ditches (Andersen et al., 2017), and in minerotrophic fens by directing upslope water flow routes back to the peatlands, including the affected areas that have not been directly drained (e.g. Ikkala et al., 2022; Isoaho et al., 2024b). Hydrological restoration raises the water table, enabling a shift towards vegetation communities which thrive in wetter conditions (Elo et al., 2025). Since these measures do not always work as intended (Isoaho et al., 2023, 2024b), every conducted measure needs to be assessed. This is currently done in the field (Similä et al., 2014; Granqvist, 2024) which is time-consuming and expensive due to the large restoration areas and remoteness of the sites, further highlighting the need for new cost-effective and spatially representative monitoring methods.

Remote sensing (RS) has been suggested as a potential tool to answer the needs for large-scale monitoring (Ikkala et al., 2026). It can produce spatiotemporally comprehensive data which can be linked to ecosystem structure and functioning. For example, drone-based methods can be used to produce accurate spatial distribution maps of vegetation patterns (Räsänen et al., 2020; Steenvoorden and Limpens, 2023) and surface wetness (Isoaho et al., 2023; Villoslada et al., 2023). However, drone flights are usually conducted in relatively small areas due to technical limitations such as battery life, and they require a field visit; thus, they do not remove the challenges related to the remoteness of the restoration sites. Instead, medium to high spatial resolution (10–30 m) satellite imagery has successfully been used for large-extent assessments (Ball et al., 2023; Isoaho et al., 2024a; Räsänen et al., 2025; Ikkala et al., 2025). While medium resolution fails to capture the spatial heterogeneity of peatlands (Steenvoorden and Limpens, 2023), it can be used to upscale the field-assessed changes in surface wetness (Burdun et al., 2023; Isoaho et al., 2024b) and vegetation (Kolari et al., 2022; Isoaho et al., 2024a; Räsänen et al., 2025). In particular, optical satellite imagery has been proven successful in capturing post-restoration changes in boreal peatlands (Isoaho et al., 2024a, 2024b; Räsänen et al., 2025). Decreases in visible, near-infrared (NIR), and shortwave-infrared (SWIR) spectral reflectance seem to indicate the increase in surface wetness (Sadeghi et al., 2015; Isoaho et al., 2023). Additionally, several moisture and vegetation indices, such as Moisture Stress Index (MSI), Normalised Difference Moisture Index (NDMI), and Normalised Difference Vegetation Index (NDVI) have been shown to correlate with peatland wetness (Meingast et al., 2014; Kalacska et al., 2018; Šimanauskienė et al., 2019; Karlqvist et al., 2024). Therefore, optical satellite data could enable straightforward peatland wetness monitoring applications.

Google Earth Engine (GEE; Gorelick et al., 2017) has emerged as a powerful tool for handling large satellite imagery datasets. It has been used for preprocessing and gathering satellite imagery for different peatland studies (Burdun et al., 2023; Isoaho et al., 2024b; Räsänen et al., 2022, 2025), and its capabilities to build applications with a simple user-interface have been demonstrated (Murray et al., 2018; Mhawej and Faour, 2020; Riggs et al., 2022; Alzurqani et al., 2024; Li and Demir, 2024; Alírio et al., 2025). GEE applications can conduct relatively complex processing steps while requiring only a few inputs from the user. However, there is a lack of GEE applications that restoration practitioners with limited technical expertise can use for restoration impact assessment in treeless boreal peatlands. In particular, applications for assessing surface wetness changes are lacking, even though hydrological monitoring has been shown to be feasible with satellite imagery. To address the above-mentioned gap, we used expert knowledge regarding peatland restoration, GEE cloud computing capabilities, and statistical methods to (1) examine which optical bands or indices detect successful hydrological restoration in treeless areas of boreal peatlands, (2) develop a user-friendly GEE application based on the results, and (3) demonstrate the usage of the application in practice.

## 2. Materials and methods

### 2.1. Study sites

We studied 24 open peatlands, mostly aapa mires, located in the middle and southern boreal regionin Finland (Fig. 1A; Table S1). The average annual temperature of the study sites (1991–2020) ranges between 2.0 and 4.9 °C whereas the average annual precipitation ranges from 604 to 703 mm (Aalto et al., 2016). All study sites are minerotrophic boreal peatlands with wet flark fen areas in the

middle and drier peatland types surrounding the wettest areas (Laitinen et al., 2005, Fig. 1B). Flark fen areas consist of water-filled depressions called flarks alternating with drier hummock strings. The vegetation of flark fens typically consist of different *Carex* and *Sphagnum* species and even some shrubs in drier strings, but the flarks can often lack vegetation cover (Räsänen and Virtanen, 2019; Kolari et al., 2022; Granlund et al., 2022). In contrast, the edge areas of the study sites are typically drier with a gradual change towards more treed peatland types.

Before restoration, all sites were mostly directly undrained, but drainage in the upper catchment and in the adjacent areas had decreased incoming surface water flows, causing changes in vegetation and surface wetness (Sallinen et al., 2019; see Fig. 1B). The sites were restored by directing water back to the peatlands with water-directing ditches, which cost-effectively reconnected the peatlands to their upper catchments (Isoaho et al., 2024b, Fig. 1B). The restoration measures were conducted between 2018 and 2023, and the first spring after restoration was defined as the start of the restoration impact.

### 2.2. Satellite imagery

We used Sentinel-2 (S2) Level 2A reflectance product and Landsat 8–9 (L8–9) Collection 2 Level-2 product within GEE from the growing seasons of 2014–2024. First, we filtered out imagery with cloud coverage of over 50 % and 30 % for S2 and L8–9, respectively, based on image metadata. Lower thresholds, such as 20–30 % are often used for S2 (e.g. Räsänen et al., 2022; Isoaho et al., 2024b). However, we wanted to maximize the number of observations, similarly to Jussila et al. (2023), as the area is characterized by frequent cloudiness which can lead to a lack of data if too low threshold is selected for image filtering. We used different cloud coverage thresholds for S2 and L8–9 because of different cloud and snow masking algorithms used for the two datasets. For S2, we used CloudScore + as it has outperformed the other state-of-the-art cloud masks and it has an operational implementation in GEE (Pasquarella et al., 2023). Based on our preliminary tests and visual interpretation, a threshold value of 0.8 in cs_cdf layer effectively masked clouds and shadows without masking many good-quality pixels. For example, a smaller value of 0.7 allowed cloud and cloud shadow borders to bypass the mask in some cases, while a value of 0.9 overly masked cloud-free pixels. As CloudScore + does not mask snow, we used Scene Layer Classification for snow masking. For L8–9, we used Quality Assessment pixels to mask all clouds, cloud shadows, and snow as CloudScore+ was available only for S2.

To improve the cross-comparability of S2 and L8–9, we harmonised the datasets. A typical approach is to use the harmonisation coefficients from the literature (e.g. Zhang et al., 2018). However, we wanted to optimise the harmonisation to open peatlands in Finland, but there were no existing coefficients available. Therefore, we empirically developed band-specific intercepts and slopes using 7500 randomly distributed 30 m radius buffers across open peatland areas in Finland (Section S1 in Supplementary material, Fig. S1, Table S2) and harmonised L8–9 to match the S2 data. Finally, to reduce spatial artefacts caused by different pixel sizes of S2 (10–20 m) and L8–9 (30 m), we resampled the L8–9 bands to the same pixel size and spacing as the S2 bands with bicubic interpolation. We note that a more comparable dataset would be constructed by e.g. average-resampling S2 to L8–9 resolutions. However, we wanted to preserve the resolution advantage of S2 for visualisation purposes as it better captures the spatial heterogeneity of peatland surface.

We used a pixel-by-pixel 40th percentile approach (Pitkänen et al., 2024) to construct cloudless and representative pre- and post-restoration satellite images. For the pre-restoration image, we used all processed images from five years prior to the first restoration-impact year (−5 to −1 years); for the post-restoration image, we used all processed images up to five years after the restoration impact (0–4 years). However, we did not include 2018 due to the prevailing drought that year (Rinne et al., 2020; Jussila et al., 2023), as extremely dry conditions would lead to a systematic shift of reflectance values. We used only those post-restoration years that were available during the study; e.g. if first restoration impact was defined as year 2023, the post-restoration image was constructed using data from years 2023 and 2024. Finally, we used data only from early summer (1 May – 15 June) to construct images with relatively wet conditions right after the snowmelt (Sallinen et al., 2023) when the restoration impacts on surface wetness are the most visible (Isoaho et al., 2024b). While this does not necessarily indicate how well the restoration functions during drier conditions in the later summer, it is still consistent with the follow-up monitoring of the peatland restoration in Finland, which is conducted during spring to assess the effectiveness of restoration measures, e.g. dam failures, in wetter conditions (Similä et al., 2014).

For the change detection of the constructed representative images, we calculated several indices widely used in peatland and wetness studies (Table 1). We also used several single bands which have been shown to be effective wetness and vegetation indicators in relatively open peatlands (Kolari et al., 2022; Isoaho et al., 2024b; Räsänen et al., 2025). We produced change maps in which the pre-restoration image was subtracted from the post-restoration image to show where the reflectance and index values had decreased or increased.

### 2.3. Statistical analyses

To assess which RS variables respond to increased surface wetness, we used three types of areas (i.e. treatments) to conduct statistical tests in our study sites (Fig. 2). To form the first and second treatment, we placed circular 30 m radius buffers at the downslope ends of the water-directing ditches (n = 199) that were further divided into successful (n = 166) and unsuccessful (n = 33) restored areas based on our visual interpretation of National Land Survey of Finland aerial imagery and expert judgment in the field. The successful ditches were able to direct water to the peatland, making the area at the end of the ditch wetter, while the unsuccessful ditches did not increase the wetness. The third treatment was constructed by randomly distributing control buffers (n = 193) of the same size in the same peatlands, with their centroids located at ≥ 300 m distance from the conducted measures, ≥50 m distance from open peatland area boundary, and ≥100 m distance from each other. It is possible that the restoration could have an effect within the control buffers, as we placed them within the restoration sites. However, recent studies have indicated that the immediate hydrological

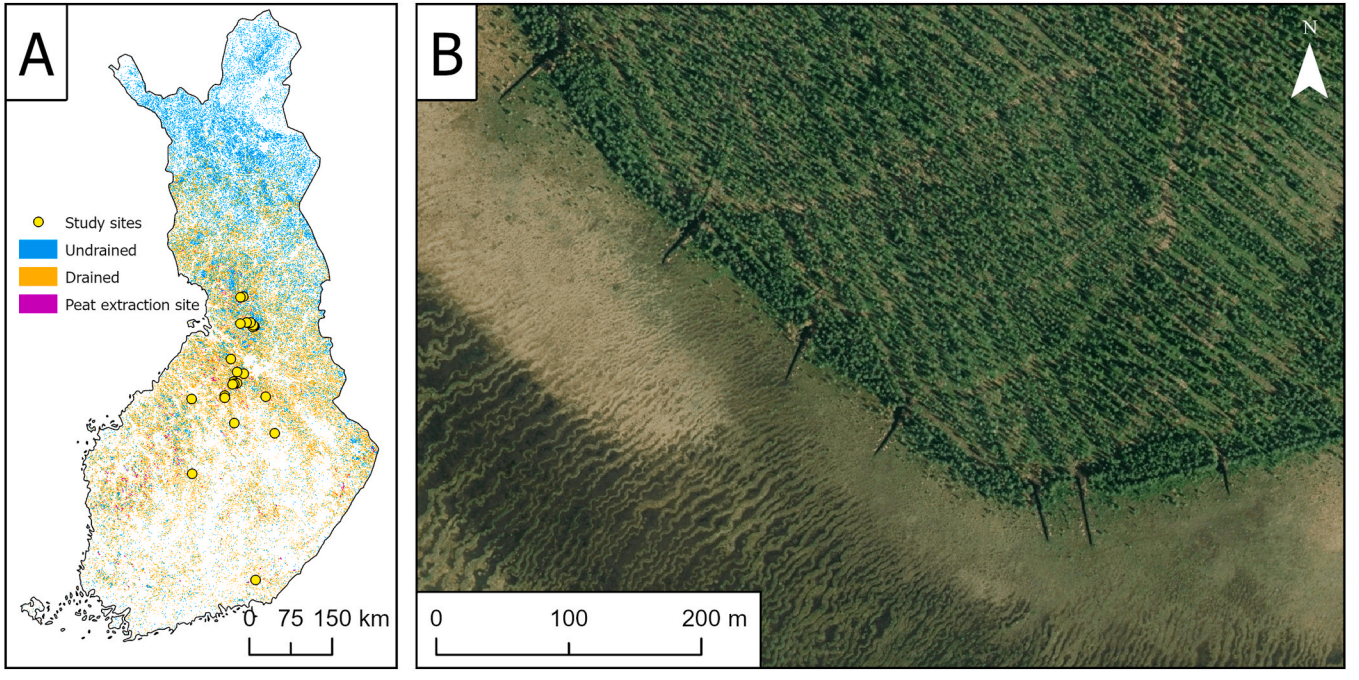


**Fig. 1.** Study site locations across Finland (A), and an example of water-directing ditches as a restoration method at Karhusuo, Pudasjärvi Finland (26.731°E, 65.473°N) (B). The ditches can be seen as narrow dark-coloured lines directing water from the upslope treed area to the open peatland. The study sites' coordinates can be found in Table S1. Peatland drainage status raster (A) is open data from Finnish Environment Institute. Background aerial image (B) is open data from National Land Survey of Finland.

**Table 1**
The used remote sensing bands and spectral indices with their equations. Justifications for the remote sensing variables are in Table S3.

| Variable | Abbreviation | Equation | Reference |
|---|---|---|---|
| Blue reflectance | Blue | | |
| Green reflectance | Green | | |
| Red reflectance | Red | | |
| Near-infrared reflectance | NIR | | |
| Shortwave infrared band 1 reflectance | SWIR1 | | |
| Shortwave infrared band 2 reflectance | SWIR2 | | |
| Shortwave infrared transformed reflectance | STR | $\frac{(1-SWIR1)^2}{2*SWIR1}$ | Sadeghi et al. (2015) |
| Normalised Difference Vegetation Index | NDVI | $\frac{NIR-RED}{NIR+RED}$ | Tucker (1979) |
| Enhanced Vegetation Index | EVI | $2.5*\frac{NIR-RED}{NIR+6*RED-7.5*Blue+1}$ | Liu and Huete (1995) |
| Soil Adjusted Vegetation Index | SAVI | $1.5*\frac{NIR-RED}{NIR+RED+0.5}$ | Huete (1988) |
| Normalised Difference Water Index | NDWI | $\frac{GREEN-NIR}{GREEN+NIR}$ | McFeeters (1996) |
| Modified Normalised Difference Water Index | MNDWI | $\frac{GREEN-SWIR2}{GREEN+SWIR2}$ | Xu (2006) |
| Normalised Difference Moisture Index | NDMI | $\frac{NIR-SWIR1}{NIR+SWIR1}$ | Gao (1996) |
| Normalised Difference Moisture Index 2 | NDMI2 | $\frac{NIR-SWIR2}{NIR+SWIR2}$ | Gao (1996) |
| Moisture Stress Index | MSI | $\frac{SWIR1}{NIR}$ | Vogelmann and Rock (1986) |

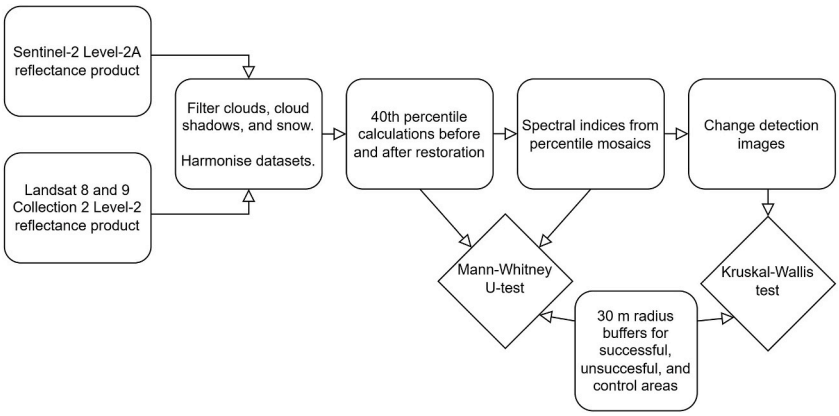


**Fig. 2.** Methodological flowchart describing the empirical study for finding optical satellite-based indicators to assess the success of hydrological peatland restoration.

impact area of water-directing ditches is relatively small (Isoaho et al., 2023, 2024b) and our sampling rules should allocate the buffers outside the immediate impacts.

We tabulated data from before- and after-restoration 40th percentile mosaics by calculating mean value of pixels within the placed buffers from each study site. For the before-after assessment and for every RS variable separately, we performed a Mann-Whitney *U* test to assess which RS variables captured changes between the before and after situations in different treatments. To find which variables best explained variation in the different treatments, we conducted a Kruskal-Wallis test using the calculated before-after difference for each RS variable. We interpreted the results of the statistical tests, i.e. p-values and test statistics, to choose which RS variables best captured the changes after restoration and differences between the treatments. We conducted statistical analyses in R (version 4.2.1; R Core Team, 2022) and created result graphs with ggplot2 package (Wickham, 2016).

## 3. Results and discussion

### *3.1. Best indicators for hydrological restoration success*

All tested variables showed statistically significant differences between pre- and post-restoration data in the successfully restored areas (Fig. 3, Table 2). In general, restoration decreased the reflectance of single bands and vegetation index values, which is consistent with e.g. Kolari et al. (2022) and Isoaho et al. (2023) who have reported a negative correlation between increased wetness and single

bands. For wetness and water indices, both increases (NDWI, MSI) and decreases (MNDWI, NDMI, NDMI2) were observed. These changes are partly consistent with e.g. Kalacska et al. (2018) who have reported negative correlation between NDMI and peatland water table, and Räsänen et al. (2025) who have shown that NDMI decreases in nutrient-rich open mires after restoration. However, in our results, MSI responded contrary to existing literature, which has indicated a negative correlation between MSI and peatland wetness (e.g. Meingast et al., 2014; Karlqvist et al., 2024).

Generally, statistical significances were stronger (p-value smaller) for single bands than for spectral indices. Additionally, only one third of the variables (NIR band, vegetation indices and NDWI) showed statistically significant differences between pre- and post-restoration situations in the unsuccessfully restored areas. This was surprising as we expected that all RS variables could detect some change in the unsuccessfully restored areas because the water-directing ditch itself should change the reflectance values within the area, even if it fails to increase the surface wetness downstream (Isoaho et al., 2023).

In the control areas, single bands did not show statistically significant differences between before- and after-restoration data, but most of the indices did. Furthermore, almost all spectral indices showed stronger statistical significance in the controls than in the unsuccessfully restored areas, while NDVI also showed a more significant change in the controls than in the successfully restored areas. Therefore, the spectral indices seem to detect changes in the control areas even though these areas should not have undergone substantial wetness changes during the monitored period. This is a surprising result, as it could be assumed that the restoration affects the reflectance within the impacted areas quite considerably; however, the reflectance in the control areas should not change substantially as immediate hydrological impacts of water-directing ditches are relatively small-scale, i.e. less than a few hundred metres from the ditch (Isoaho et al., 2024b). In the future research, it could be studied if the vegetation indices might capture slow vegetation changes during the monitoring window.

The highest H-statistic value from the Kruskal-Wallis test (i.e. the largest difference between the treatments) was achieved for the

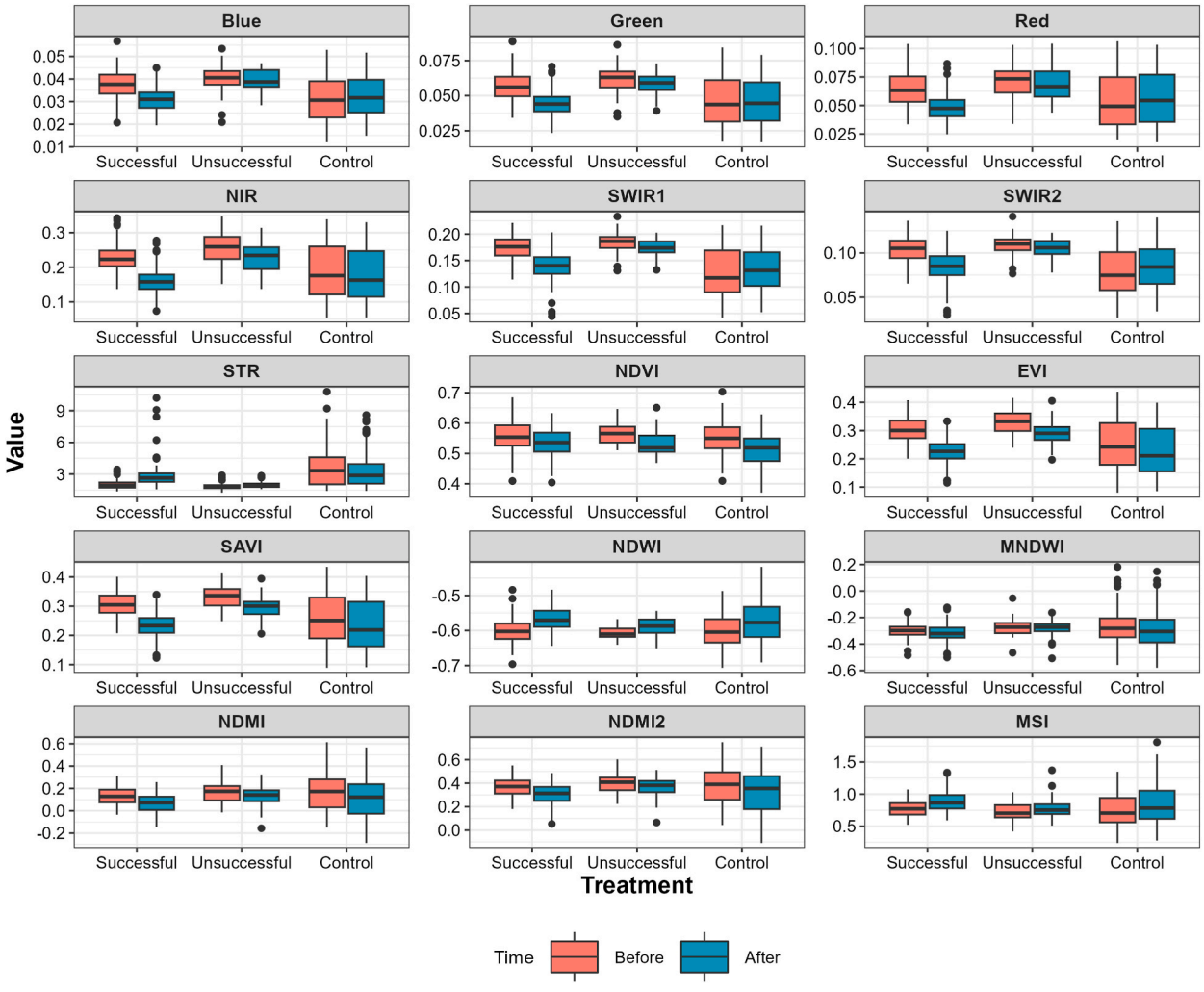


**Fig. 3.** Boxplots of spectral bands and indices across different treatments before and after restoration. Abbreviations are explained in Table 1. Each boxplot contains reflectance or index values extracted from a 30 m radius buffer area before (red) and after restoration (blue).

**Table 2**
Mann-Whitney *U* test p-values in scientific notations between before- and after-restoration time windows with different variables and treatments. Stars indicate *p < 0.05, **p < 0.01, ***p < 0.001, and ****p < 0.0001. Abbreviations are explained in Table 1.

| Variable | Successful | Unsuccessful | Control |
|---|---|---|---|
| Blue | 1.9E-19**** | 5.1E-01 | 2.2E-01 |
| Green | 8.3E-27**** | 1.3E-01 | 9.7E-01 |
| Red | 4.9E-23**** | 4.4E-01 | 3.6E-01 |
| NIR | 4.7E-35**** | 4.0E-02* | 1.2E-01 |
| SWIR1 | 1.7E-29**** | 5.6E-02 | 2.8E-01 |
| SWIR2 | 5.7E-24**** | 1.8E-01 | 9.3E-02 |
| STR | 1.7E-29**** | 5.6E-02 | 2.8E-01 |
| NDVI | 5.6E-05**** | 3.8E-04*** | 2.2E-10**** |
| EVI | 5.0E-33**** | 1.1E-03** | 7.0E-03** |
| SAVI | 8.6E-33**** | 1.2E-03** | 6.1E-03** |
| NDWI | 4.8E-18**** | 1.5E-03** | 1.2E-05**** |
| MNDWI | 4.5E-03** | 8.5E-01 | 5.1E-02 |
| NDMI | 3.6E-09**** | 2.7E-01 | 3.9E-03** |
| NDMI2 | 4.9E-10**** | 2.3E-01 | 1.8E-03** |
| MSI | 3.6E-09**** | 2.7E-01 | 3.9E-03** |

NIR band by a relatively large margin over the second highest-scoring variable (SWIR1; Fig. 4). NIR and SWIR1 were followed by the rest of the single bands, STR, SAVI, and EVI. The rest of the spectral indices had considerably smaller H-statistics, while MNDWI did not have a statistically significant result (p-value was >0.05). Generally, these results indicate that NIR and SWIR1 best captured variation in the before-after differences in the different treatments. Furthermore, other spectral bands showed a similar but weaker impact than NIR and SWIR1. Spectral wetness indices seemed to work poorly as they captured differences between the treatments with small H-statistics. In contrast, vegetation indices EVI and SAVI worked quite similarly to the single bands. This has also been observed in previous studies, indicating that spectral wetness indices do not necessarily work as wetness indicators in boreal aapa mires as successfully as the single bands (Kolari et al., 2022; Isoaho et al., 2024b; Keränen et al., 2024). Overall, the results imply that the single bands work better than the spectral indices when assessing the immediate hydrological restoration impact in treeless boreal peatlands.

Previous studies have emphasized the importance of the NIR region for monitoring aapa mire wetness (Kolari et al., 2022; Keränen et al., 2024). This is also supported by our results, which further confirms that single bands can best detect spatial and temporal wetness changes. Additionally, the SWIR region has been associated with wetness changes in boreal peatlands (Räsänen et al., 2022; Jussila et al., 2023; Isoaho et al., 2024b). While NIR seemed to work best in our case, SWIR1 also quite well detected variation between the treatments. Therefore, if only two variables were chosen, NIR and SWIR1 would be the best indicators for assessing spatial restoration success of surface wetness in open parts of boreal aapa mires.

### 3.2. Description of google earth engine application

We developed a GEE application based on the results of the statistical tests and incorporated the best performing satellite variables (NIR and SWIR1) as indicators of the restoration impact into the application. The application uses the same approach for collecting and processing S2 and L8–9 imagery as described in Section 2.2. The application operates through a user-friendly interface in which the user defines (1) an area of interest using a point and (2) the year of the first spring after the restoration (Fig. 5). The user can choose

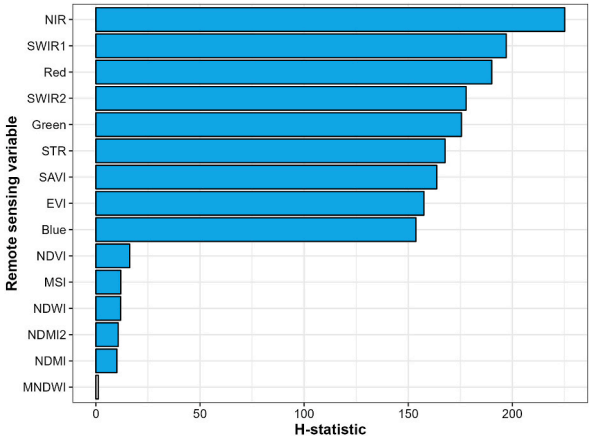


**Fig. 4.** Kruskal-Wallis H-statistics of optical bands and indices between the difference (after - before) and treatments. Blue bars are statistically significant H-statistics (p-value <0.05) and the white bar (MNDWI) is not. Abbreviations are explained in Table 1.

whether they want to use the harmonisation coefficients for Finnish open peatlands developed in this study (Table S2) or the general coefficients developed for global applications based on data from southern Africa (Zhang et al., 2018). While we did not test the global coefficients in the empirical study, it is worth noting that S2 covers most of the data and L8–9 only supplements it (see Table S4); therefore, the differences in representative images between the two harmonisation options are probably quite small. Executing the application generates representative false-colour images for the situations before and after restoration (i.e. the user-defined year) as well as NIR- and SWIR1-change images, by default within a 3 km radius buffer around the user-defined point. The buffer radius can be changed in the user interface. Additionally, the application produces time series plots of the NIR and SWIR1 values from 1 May to 31 August each year from 2014 to the present, using a 30 m radius buffer around the user-defined point.

### 3.3. Demonstration of application

Here, we show the usage of the application with the sites Peurasuo (first restoration-impacted year 2021), Karhusuo (2022), Pesäneva (2023), and Törmäisenrimpi (2024; Fig. 6) selected from our original sample of 24 sites (Fig. 1, Table S1). We chose these sites to show how different restoration years and outcomes affect the results and to demonstrate the use of the application in restored boreal peatlands. At Peurasuo, the restoration measures included ditch infilling in addition to water-directing ditches, and at all sites except Pesäneva, tree felling was also carried out outside the open peatland area.

The GEE application results revealed spatial variation in restoration effects (Fig. 7). Some of the restoration measures had relatively large impact areas, while others showed increased surface wetness only within a limited spatial extent. Some systematic changes in the reflectance values caused by annual variation could also be seen. In Peurasuo, water-directing measures decreased NIR and SWIR1 reflectance broadly in the northeastern part of the site. Other parts of the site experienced fewer changes but e.g. the western areas, which have undergone ditch infilling, changed similarly to the areas affected by water-directing ditches. In Karhusuo, water-directing measures showed clear reflectance decrease patterns in the ditch-impacted areas, while the rest of the site had increases in reflectance, except for some areas close to a pond in the southeast corner of the area. In Pesäneva, the water-directing measures in the eastern part of the site seemed to have a spatially extensive impact area, as did the westernmost directing measure. Two measures in the south seemed not to have worked as intended. Additionally, there were clear changes in the northwestern part of the site even though no restoration measures were nearby. In Törmäsenrimpi, both water-directing ditches seem to have decreased the reflectance; especially, the western one had a relatively large impact area (approximately 5 ha) based on visual interpretation.

Overall, the developed GEE application can be used to determine (1) if a restoration measure has successfully increased the surface wetness of the site, and (2) the spatial extent of the restoration-impacted area. This semi-automated procedure is particularly beneficial for restoration practitioners who need to assess whether specific restoration measures work as intended. For example, Metsähallitus Parks & Wildlife Finland, which implements peatland restoration on nature conservation areas owned by the Finnish state, instructs that follow-up monitoring needs to be conducted in every restoration site (Similä et al., 2014). Additionally, the nature restoration law requires active post-restoration monitoring (Regulation (EU) 2024/1991). Therefore, the developed application can significantly improve the quantification of the extent of restoration impact areas and help with the planning of field assessments, thereby saving resources. In addition, the application can be used by landowners and other stakeholders who are interested in peatland restoration as well as in its spatial impacts and outcomes.

Although we focused on the restoration impacts of water-directing ditches in open peatlands, we have also noticed that the developed application can, to some extent, detect the rewetting effects of damming and filling of drainage ditches in partly treed peatlands (Fig. 7, western part of Peurasuo). This could also enable a more general assessment of mire restoration, but these results must be interpreted with caution, as this aspect should be further developed and tested. The application can also potentially be applied to detect post-rewetting changes in other open landscapes such as agricultural peatlands and peat extraction sites (Andersen et al., 2017; Chimner et al., 2017).

The information provided by the application can also be supplemented by field observations. This connection can be bidirectional: either the application identifies the locations that need to be checked in the field or the application is used to quantify the spatial extent of the changes observed in the field (Isoaho et al., 2024c). In both cases, the use of our GEE application provides a fast approach and substantial assistance for evaluating restoration success.

### 3.4. Limitations and outlook

We have shown that satellite imagery is suitable for monitoring the restoration of open mires. However, our study also has its own limitations. We conducted tests only in Finland as we wanted to focus on developing an application that works for Finnish practitioners. This means that results from other parts of the boreal zone and especially other biogeographic regions need to be interpreted with caution. Additionally, sites to be studied with our method need to be relatively treeless and possibly relatively wet. Tree cover hides the peatland surface, which limits wetness monitoring (Burdun et al., 2023), and the relationship between water table and remote sensing proxies diminishes when the water table decreases too deep due to the loss of capillary connections (Asmuβ et al., 2019; Burdun et al., 2023; Ikkala et al., 2025). This further limits the applicability across different peatland sites and types.

Interpreting surface wetness changes can also be challenging. Increased wetness is often visible as inundated surfaces, which are easily observed in the images, but in some cases, the increase in wetness occurs below the peatland surface. In the latter cases, the peatland surface often appears darker, but not always (i.e. the reflectance is not necessarily lower) after increased wetness (Chasmer et al., 2020; Kolari et al., 2022; Isoaho et al., 2023). This complicates the analysis and emphasises the need for additional information about the site and its vegetation to obtain a more reliable interpretation of the images.

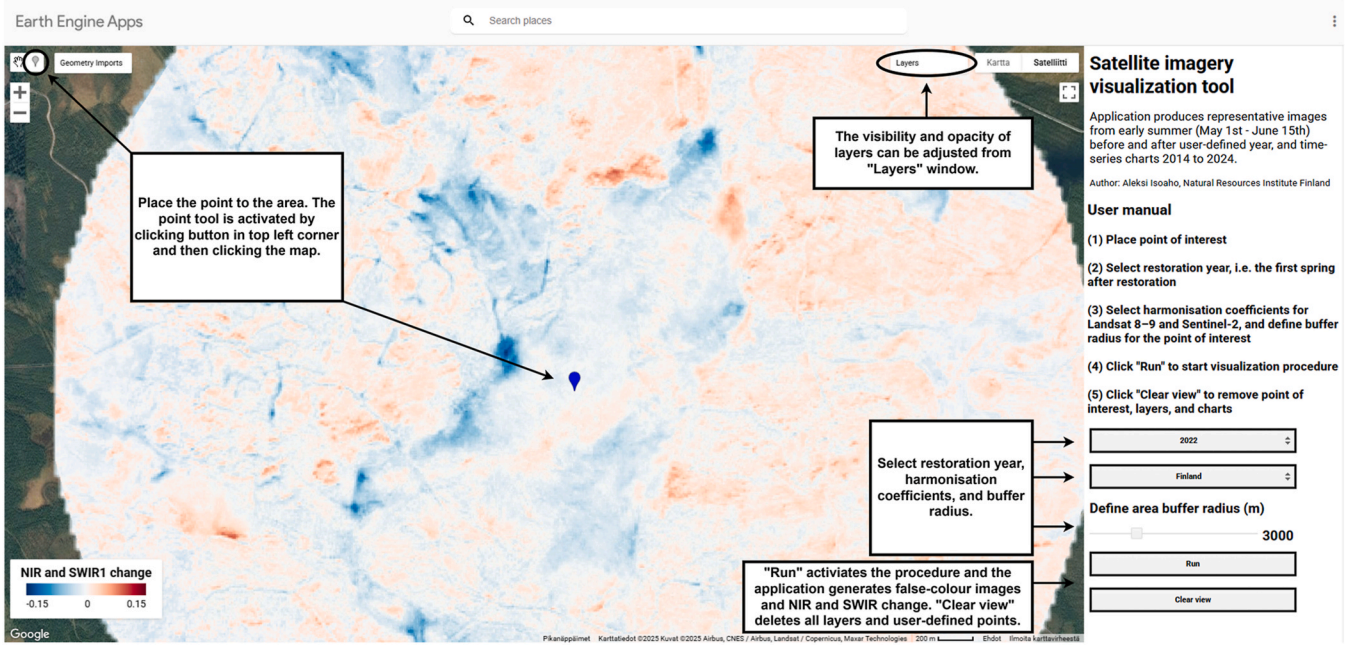


**Fig. 5.** Snapshot of the application with textboxes explaining how the application is used. The analysed peatland site is Makkarasuo (26.166°E, 64.993°N), which was one of our study sites in the empirical study (Section 2).

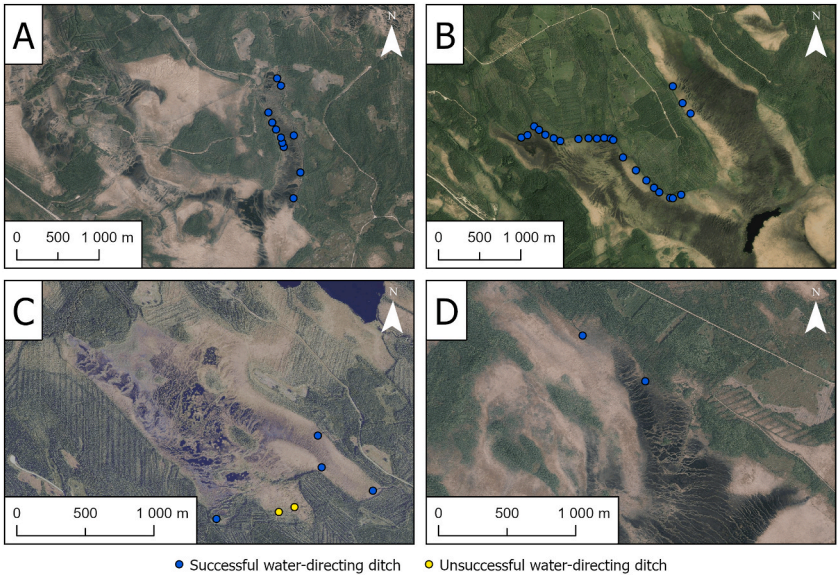


**Fig. 6.** Selected sites for demonstration labelled as Peurasuo (26.511°E, 64.075°N) (A), Karhusuo (26.731°E, 65.473°N) (B), Pesäneva (24.854°E, 63.799°N) (C), and Törmäsenrimpi (26.516°E, 64.252°N) (D). Background aerial images are open data from National Land Survey of Finland.

In the future, more satellite-based variables could be tested for assessing hydrological restoration success. For example, we did not test the usability of optical trapezoid model (OPTRAM; Sadeghi et al., 2017) because it requires local parameterisation. While Räsänen et al. (2022) and Burdun et al. (2023) have highlighted its functionality with temporal water table dynamics in boreal peatlands, local parameterisation leads to variation in value ranges between different sites. Therefore, OPTRAM dynamics are not globally comparable, which hampers OPTRAM's usability in automated applications with a predefined visualisation palette and range. Moreover, widely inundated areas, such as flark fens in aapa mires, are not suitable for OPTRAM (Sadeghi et al., 2017). While OPTRAM-2 was developed to overcome the gap in inundated areas (Sadeghi et al., 2023), it still requires additional local calibrations, making it less suitable for the developed application.

Additionally, we did not test Sentinel-1 C-band synthetic aperture radar (SAR) imagery for the change detection. While previous studies have shown that SAR backscatter is connected to peatland water table dynamics (Bechtold et al., 2018; Asmuβ et al., 2019), optical imagery has outperformed it in studies conducted in boreal peatlands (Räsänen et al., 2022; Isoaho et al., 2024b). Furthermore, SAR backscatter does not change linearly: increased wetness first increases the amount of backscatter up to inundation, after which the backscatter drastically decreases due to specular reflection (Sass and Creed, 2008; Schultz et al., 2023). In the wettest parts of boreal aapa mires, the water level is above the peatland surface or restoration can sharply raise the water onto the surface (Menberu et al., 2016; Isoaho et al., 2024b), making change detection with SAR suboptimal for restoration impact assessment.

Further complexity for the change detection approach arises from the fact that NIR reflectance is linked not only to wetness but also to the greenness of the vegetation. Kolari et al. (2022) studied a case where a flark fen area in an aapa mire gradually became overgrown with mire vegetation dominated by *Sphagnum* mosses. The site remained wet, but NIR levels increased as open water surfaces became covered with vegetation. This must also be considered when studying the effects of restoration. As we have shown above, a decrease in NIR reflectance indicates an increase in surface wetness and, therefore, the success of hydrological restoration. However, the increased wetness is expected to be followed by a vegetation recovery (Elo et al., 2025), which in turn can potentially be seen as an increase in NIR reflectance (Räsänen et al., 2025). This change can be mistakenly interpreted as a drying of the mire, although it is an important part of the restoration process.

Finally, we highlight that the application was developed for assessing hydrological impact during peak wetness. This best enables the practitioners to assess whether hydrological restoration measures work as intended (Similä et al., 2014). From an ecohydrological perspective, the monitoring of drought periods from midsummer could be more interesting as restored forestry-drained peatlands have been observed to be hydrologically less resilient than pristine mires (Ikkala and Similä, 2024). However, changes in deep water tables might be very difficult to monitor with remote sensing as discussed above.

## 4. Conclusion

We have assessed different optical satellite variables for peatland restoration impact assessment of boreal treeless sites and developed a GEE application based on our results. We have demonstrated that single bands, especially NIR and SWIR1, detect hydrological restoration impact areas better than other optical RS variables. The developed application has a user-friendly interface to enable access for users with limited RS knowledge. It generates and shows representative before and after false colour images as well as change images in NIR and SWIR1 bands. The application is ready to be used in operational aapa mire restoration impact assessments

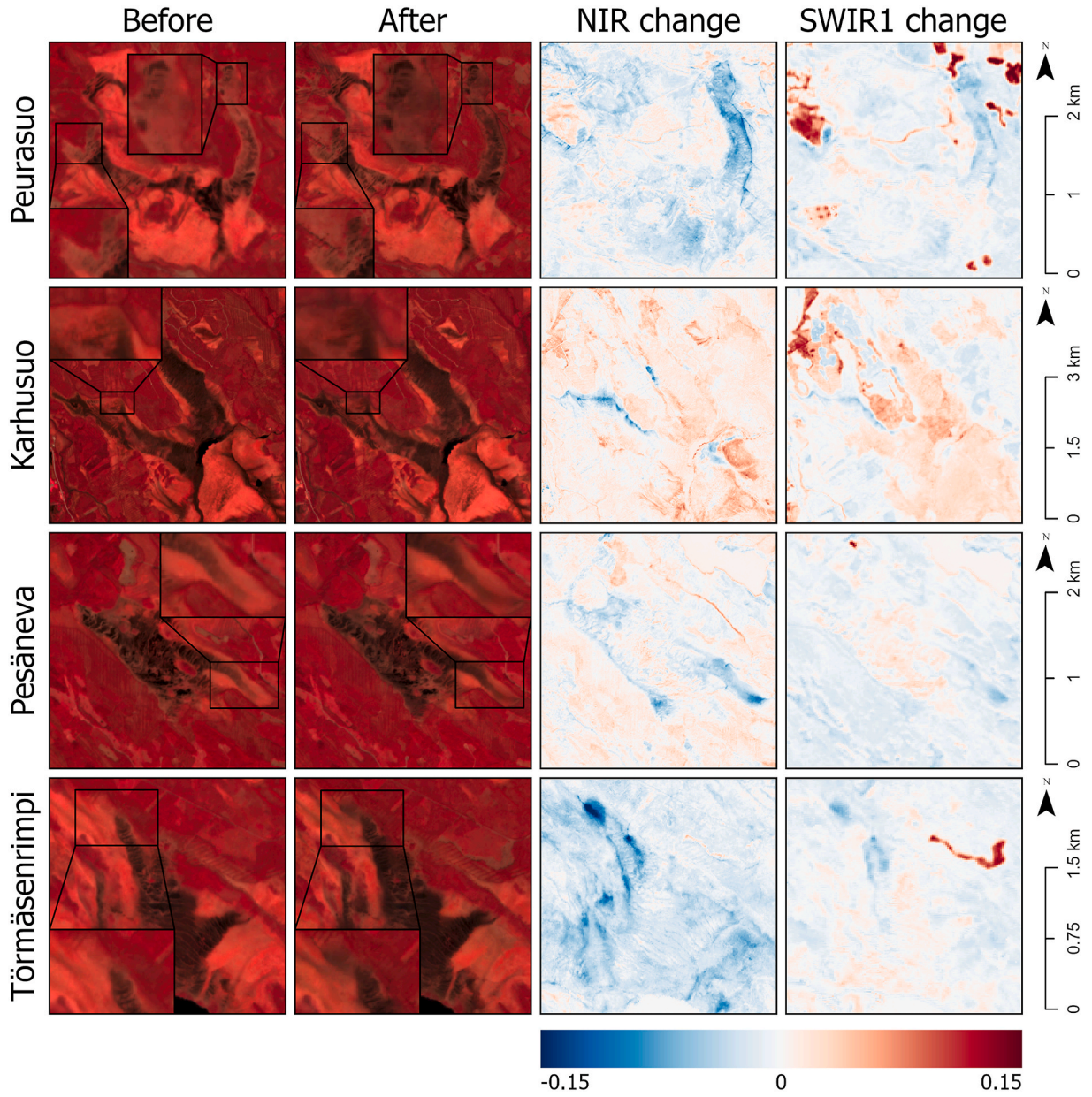


**Fig. 7.** Restoration impacts in the demonstration sites (see Fig. 6). The representative before and after restoration images (on the left) are false-colour visualisations built with NIR, Red, and Green bands. The band-specific change images are shown on the right. In general, increased wetness in open peatland area decreases reflectance (darker areas in the false-colour images, see the zoomed examples; negative NIR or SWIR changes shown as blue). The developed Google Earth Engine application uses the same visualisation styles. Note that the representative post-restoration images here include data up to June 15, 2024.

and could be further tested and developed for monitoring the restoration of other types of peatlands and ecosystems.

## CRediT authorship contribution statement

**Aleksi Isoaho:** Writing – original draft, Visualization, Validation, Software, Methodology, Investigation, Formal analysis, Data curation, Conceptualization. **Timo P. Pitkänen:** Writing – review & editing, Software. **Lauri Ikkala:** Writing – review & editing, Investigation. **Antti Sallinen:** Writing – review & editing, Investigation. **Parvez Rana:** Writing – review & editing, Investigation. **Hannu Marttila:** Writing – review & editing, Funding acquisition. **Lassi Päkkilä:** Writing – review & editing. **Aleksi Räsänen:** Writing – review & editing, Project administration, Funding acquisition, Conceptualization.

## Software availability

Application can be found at: https://aleksiisoaho.users.earthengine.app/view/optical-satellite-before-after-visualisation.

## Declaration of competing interest

The authors declare that they have no known competing financial interests or personal relationships that could have appeared to influence the work reported in this paper.

## Acknowledgements

This study was funded by the Ministry of Environment, Finland (VN/14352/2022) and European Union LIFE programme (LIFE22-IPN-FI-Priodiversity LIFE). We thank the Finnish Expert Group on Peatland Restoration (part of the Finnish Board on Ecological Restoration) for fruitful discussions and Juha Jämsen for providing the locations of some of the restoration sites.

## Appendix A. Supplementary data

Supplementary data to this article can be found online at https://doi.org/10.1016/j.rsase.2025.101836.

## Data availability

Data will be made available on request.

## References

Aalto, J., Pirinen, P., Jylhä, K., 2016. New gridded daily climatology of Finland: permutation-based uncertainty estimates and temporal trends in climate. J. Geophys. Res. Atmospheres. 121, 3807–3823. https://doi.org/10.1002/2015JD024651.

Alírio, J., Garcia, N., Campos, J.C., Arenas-Castro, S., Pôças, I., Duarte, L.B., Teodoro, A.C., Sillero, N., 2025. Montrends: a google Earth engine application for analysing species' habitat suitability over time. Ecol. Inform. 89, 103201. https://doi.org/10.1016/j.ecoinf.2025.103201.

Alzurqani, S.A., Zurqani, H.A., White, D., Bridges, K., Jackson, S., 2024. Google Earth engine application for mapping and monitoring drought patterns and trends: a case study in Arkansas, USA. Ecol. Indic. 168, 112759. https://doi.org/10.1016/j.ecolind.2024.112759.

Andersen, R., Farrell, C., Graf, M., Muller, F., Calvar, E., Frankard, P., Caporn, S., Anderson, P., 2017. An overview of the progress and challenges of peatland restoration in Western Europe: peatland restoration in Western Europe. Restor. Ecol. 25, 271–282. https://doi.org/10.1111/rec.12415.

Asmuß, T., Bechtold, M., Tiemeyer, B., 2019. On the potential of Sentinel-1 for high resolution monitoring of water table dynamics in grasslands on organic soils. Remote Sens. 11, 1659. https://doi.org/10.3390/rs11141659.

Ball, J., Gimona, A., Cowie, N., Hancock, M., Klein, D., Donaldson-Selby, G., Artz, R.R.E., 2023. Assessing the potential of using Sentinel-1 and 2 or high-resolution aerial imagery data with machine learning and data science techniques to model peatland restoration progress – a northern Scotland case study. Int. J. Rem. Sens. 44, 2885–2911. https://doi.org/10.1080/01431161.2023.2209916.

Bechtold, M., Schlaffer, S., Tiemeyer, B., De Lannoy, G., 2018. Inferring water table depth dynamics from ENVISAT-ASAR C-Band backscatter over a range of peatlands from deeply-drained to natural conditions. Remote Sens. 10, 536. https://doi.org/10.3390/rs10040536.

Bonn, A., Allott, T., Evans, M., Joosten, H., Stoneman, R. (Eds.), 2016. Peatland Restoration and Ecosystem Services: Science, Policy and Practice, first ed. Cambridge University Press. https://doi.org/10.1017/CBO9781139177788.

Burdun, I., Bechtold, M., Aurela, M., De Lannoy, G., Desai, A.R., Humphreys, E., Kareksela, S., Komisarenko, V., Liimatainen, M., Marttila, H., Minkkinen, K., Nilsson, M.B., Ojanen, P., Salko, S.-S., Tuittila, E.-S., Uuemaa, E., Rautiainen, M., 2023. Hidden becomes clear: optical remote sensing of vegetation reveals water table dynamics in northern peatlands. Remote Sens. Environ. 296, 113736. https://doi.org/10.1016/j.rse.2023.113736.

Chasmer, L., Mahoney, C., Millard, K., Nelson, K., Peters, D., Merchant, M., Hopkinson, C., Brisco, B., Niemann, O., Montgomery, J., Devito, K., Cobbaert, D., 2020. Remote sensing of boreal wetlands 2: methods for evaluating boreal wetland ecosystem state and drivers of change. Remote Sens. 12, 1321. https://doi.org/10.3390/rs12081321.

Chimner, R.A., Cooper, D.J., Wurster, F.C., Rochefort, L., 2017. An overview of peatland restoration in North America: where are we after 25 years? Restor. Ecol. 25, 283–292. https://doi.org/10.1111/rec.12434.

Elo, M., Isoaho, A., Korhonen, P., Marttila, H., Ovaskainen, O., Päkkilä, L., Rana, P., Räsänen, A., 2025. Relationship between hydrological restoration and the recovery of vegetation communities in boreal forestry-drained peatlands. J. Appl. Ecol., 70197 https://doi.org/10.1111/1365-2664.70197, 1365-2664.

Gann, G.D., McDonald, T., Walder, B., Aronson, J., Nelson, C.R., Jonson, J., Hallett, J.G., Eisenberg, C., Guariguata, M.R., Liu, J., Hua, F., Echeverría, C., Gonzales, E., Shaw, N., Decleer, K., Dixon, K.W., 2019. International principles and standards for the practice of ecological restoration. In: Restor. Ecol., second ed., vol. 27. https://doi.org/10.1111/rec.13035

Gao, B., 1996. NDWI—A normalized difference water index for remote sensing of vegetation liquid water from space. Remote Sens. Environ. 58, 257–266. https://doi.org/10.1016/S0034-4257(96)00067-3.

Gorelick, N., Hancher, M., Dixon, M., Ilyushchenko, S., Thau, D., Moore, R., 2017. Google Earth engine: planetary-scale geospatial analysis for everyone. Remote Sens. Environ. 202, 18–27. https://doi.org/10.1016/j.rse.2017.06.031.

Granlund, L., Vesakoski, V., Sallinen, A., Kolari, T.H.M., Wolff, F., Tahvanainen, T., 2022. Recent lateral expansion of sphagnum bogs over central Fen areas of boreal aapa mire complexes. Ecosystems 25, 1455–1475. https://doi.org/10.1007/s10021-021-00726-5.

Granqvist, A.-L., 2024. Vesienpalautus suojelusoille : opas käytännön toimijoille. Etelä-Pohjanmaan ELY-keskus 09/2024.

Harris, L.I., Richardson, K., Bona, K.A., Davidson, S.J., Finkelstein, S.A., Garneau, M., McLaughlin, J., Nwaishi, F., Olefeldt, D., Packalen, M., Roulet, N.T., Southee, F. M., Strack, M., Webster, K.L., Wilkinson, S.L., Ray, J.C., 2022. The essential carbon service provided by northern peatlands. Front. Ecol. Environ. 20, 222–230. https://doi.org/10.1002/fee.2437.

Heikkinen, R.K., Aapala, K., Määttänen, A.-M., Leikola, N., Kartano, L., Aalto, J., 2023. Climate change and land use threats to species of aapa mires, an EU priority habitat. J. Nat. Conserv. 73, 126390. https://doi.org/10.1016/j.jnc.2023.126390.

Holden, J., Evans, M.G., Burt, T.P., Horton, M., 2006. Impact of land drainage on peatland hydrology. J. Environ. Qual. 35, 1764–1778. https://doi.org/10.2134/jeq2005.0477.

Huete, A.R., 1988. A soil-adjusted vegetation index (SAVI). Remote Sens. Environ. 25, 295–309. https://doi.org/10.1016/0034-4257(88)90106-X.
Ikkala, L., Ismail, Wolff, F., Marttila, H., Ronkanen, A.-K., Alekseychik, P., Rana, P., Kohv, M., Tahvanainen, T., Tolvanen, A., Haghighi, A.T., Kumpula, T., Osborne, C., Ilmonen, J., Haapalehto, T., Kløve, B., Räsänen, A., 2025. Remote sensing applications for monitoring restoration outcomes in boreal forestry-drained peatlands - reviewed applications and future potential. Remote Sens. Environ. 333, 115093. https://doi.org/10.1016/j.rse.2025.115093.
Ikkala, L., Ronkanen, A.-K., Ilmonen, J., Similä, M., Rehell, S., Kumpula, T., Päkkilä, L., Klöve, B., Marttila, H., 2022. Unmanned aircraft system (UAS) structure-from-motion (SfM) for monitoring the changed flow paths and wetness in minerotrophic peatland restoration. Remote Sens. 14, 3169. https://doi.org/10.3390/rs14133169.
Ikkala, L., Similä, M., 2024. Proposals for developing the monitoring of restored peatlands – experiences gained in hydrology LIFE project for developing general and hydrological monitoring as well as setting up monitoring by remote sensing. Metsähallituksen luonnonsuojelujulkaisuja. Sarja A 253.
Isoaho, A., Elo, M., Marttila, H., Rana, P., Lensu, A., Räsänen, A., 2024a. Monitoring changes in boreal peatland vegetation after restoration with optical satellite imagery. Sci. Total Environ. 957, 177697. https://doi.org/10.1016/j.scitotenv.2024.177697.
Isoaho, A., Ikkala, L., Marttila, H., Hjort, J., Kumpula, T., Korpelainen, P., Räsänen, A., 2023. Spatial water table level modelling with multi-sensor unmanned aerial vehicle data in boreal aapa mires. Remote Sens. Appl. Soc. Environ. 32, 101059. https://doi.org/10.1016/j.rsase.2023.101059.
Isoaho, A., Ikkala, L., Päkkilä, L., Marttila, H., Kareksela, S., Räsänen, A., 2024b. Multi-sensor satellite imagery reveals spatiotemporal changes in peatland water table after restoration. Remote Sens. Environ. 306, 114144. https://doi.org/10.1016/j.rse.2024.114144.
Isoaho, A., Ikkala, L., Räsänen, A., 2024c. Prioritising restoration monitoring of aapa mires using satellite image change detection. Suo - Mires Peat 75, 49–62.
Jussila, T., Heikkinen, R.K., Anttila, S., Aapala, K., Kervinen, M., Aalto, J., Vihervaara, P., 2023. Quantifying wetness variability in aapa mires with Sentinel-2: towards improved monitoring of an EU priority habitat. Remote Sens. Ecol. Conserv, rse2.363. https://doi.org/10.1002/rse2.363.
Kalacska, M., Arroyo-Mora, J., Soffer, R., Roulet, N., Moore, T., Humphreys, E., Leblanc, G., Lucanus, O., Inamdar, D., 2018. Estimating peatland water table depth and net ecosystem exchange: a comparison between satellite and airborne imagery. Remote Sens. 10, 687. https://doi.org/10.3390/rs10050687.
Karlqvist, S., Burdun, I., Salko, S.-S., Juola, J., Rautiainen, M., 2024. Retrieval of moisture content of common sphagnum peat moss species from hyperspectral and multispectral data. Remote Sens. Environ. 315, 114415. https://doi.org/10.1016/j.rse.2024.114415.
Keränen, K., Isoaho, A., Räsänen, A., Hjort, J., Kumpula, T., Korpelainen, P., Rana, P., 2024. Multi-resolution remote sensing for flark area detection in boreal aapa mires. Int. J. Rem. Sens. 45, 4324–4343. https://doi.org/10.1080/01431161.2024.2359732.
Kolari, T.H.M., Sallinen, A., Wolff, F., Kumpula, T., Tolonen, K., Tahvanainen, T., 2022. Ongoing fen–bog transition in a boreal aapa mire inferred from repeated field sampling, aerial images, and landsat data. Ecosystems 25, 1166–1188. https://doi.org/10.1007/s10021-021-00708-7.
Laine, J., Laiho, R., Minkkinen, K., Vasander, H., 2006. Forestry and boreal peatlands. In: Wielder, K., Vitt, D. (Eds.), Boreal Peatland Ecosystems, Ecological Studies. Springer, Berlin, Heidelberg.
Laitinen, J., Rehell, S., Huttunen, A., 2005. Vegetation-related hydrotopographic and hydrologic classification for aapa mires (hirvisuo, Finland). Ann. Bot. Fenn. 42, 107–121.
Leifeld, J., Menichetti, L., 2018. The underappreciated potential of peatlands in global climate change mitigation strategies. Nat. Commun. 9, 1071. https://doi.org/10.1038/s41467-018-03406-6.
Li, Z., Demir, I., 2024. MultiRS flood mapper: a google earth engine application for water extent mapping with multimodal remote sensing and quantile-based postprocessing. Environ. Model. Software 176, 106022. https://doi.org/10.1016/j.envsoft.2024.106022.
Liu, H.Q., Huete, A., 1995. A feedback based modification of the NDVI to minimize canopy background and atmospheric noise. IEEE Trans. Geosci. Rem. Sens. 33, 457–465. https://doi.org/10.1109/TGRS.1995.8746027.
Maanavilja, L., Aapala, K., Haapalehto, T., Kotiaho, J.S., Tuittila, E.-S., 2014. Impact of drainage and hydrological restoration on vegetation structure in boreal spruce swamp forests. For. Ecol. Manag. 330, 115–125. https://doi.org/10.1016/j.foreco.2014.07.004.
McFeeters, S.K., 1996. The use of the Normalized difference water index (NDWI) in the delineation of open water features. Int. J. Rem. Sens. 17, 1425–1432. https://doi.org/10.1080/01431169608948714.
Meingast, K.M., Falkowski, M.J., Kane, E.S., Potvin, L.R., Benscoter, B.W., Smith, A.M.S., Bourgeau-Chavez, L.L., Miller, M.E., 2014. Spectral detection of near-surface moisture content and water-table position in northern peatland ecosystems. Remote Sens. Environ. 152, 536–546. https://doi.org/10.1016/j.rse.2014.07.014.
Menberu, M.W., Haghighi, A.T., Ronkanen, A., Marttila, H., Kløve, B., 2018. Effects of drainage and subsequent restoration on peatland hydrological processes at catchment scale. Water Resour. Res. 54, 4479–4497. https://doi.org/10.1029/2017WR022362.
Menberu, M.W., Tahvanainen, T., Marttila, H., Irannezhad, M., Ronkanen, A.-K., Penttinen, J., Kløve, B., 2016. Water-table-dependent hydrological changes following peatland forestry drainage and restoration: analysis of restoration success. Water Resour. Res. 52, 3742–3760. https://doi.org/10.1002/2015WR018578.
Mhawej, M., Faour, G., 2020. Open-source google Earth engine 30-m evapotranspiration rates retrieval: the SEBALIGEE system. Environ. Model. Software 133, 104845. https://doi.org/10.1016/j.envsoft.2020.104845.
Minkkinen, K., Byrne, K., Trettin, C., 2008. Climate impacts of peatland forestry. In: Strack, M. (Ed.), Peatlands and Climate Change. International Peatland Society.
Murray, N.J., Keith, D.A., Simpson, D., Wilshire, J.H., Lucas, R.M., 2018. Remap : an online remote sensing application for land cover classification and monitoring. Methods Ecol. Evol. 9, 2019–2027. https://doi.org/10.1111/2041-210X.13043.
Pasquarella, V.J., Brown, C.F., Czerwinski, W., Rucklidge, W.J., 2023. Comprehensive quality assessment of optical satellite imagery using weakly supervised video learning. In: 2023 IEEE/CVF Conference on Computer Vision and Pattern Recognition Workshops (CVPRW). Presented at the 2023 IEEE/CVF Conference on Computer Vision and Pattern Recognition Workshops (CVPRW). IEEE, Vancouver, BC, Canada, pp. 2125–2135. https://doi.org/10.1109/CVPRW59228.2023.00206.
Pitkänen, T.P., Balazs, A., Tuominen, S., 2024. Automatized Sentinel-2 mosaicking for large area forest mapping. Int. J. Appl. Earth Obs. Geoinformation 127, 103659. https://doi.org/10.1016/j.jag.2024.103659.
R Core Team, 2022. R: a Language and Environment for Statistical Computing. R Foundation for Statistical Computing.
Ramchunder, S.J., Brown, L.E., Holden, J., 2012. Catchment-scale peatland restoration benefits stream ecosystem biodiversity. J. Appl. Ecol. 49, 182–191. https://doi.org/10.1111/j.1365-2664.2011.02075.x.
Räsänen, A., Aurela, M., Juutinen, S., Kumpula, T., Lohila, A., Penttilä, T., Virtanen, T., 2020. Detecting northern peatland vegetation patterns at ultra-high spatial resolution. Remote Sens. Ecol. Conserv. 6, 457–471. https://doi.org/10.1002/rse2.140.
Räsänen, A., Jantunen, A., Isoaho, A., Ikkala, L., Rana, P., Marttila, H., Elo, M., 2025. Changes in satellite-derived spectral variables and their linkages with vegetation changes after peatland restoration. Restor. Ecol. 33, e14338. https://doi.org/10.1111/rec.14338.
Räsänen, A., Kekkonen, H., Lehtonen, H., Miettinen, A., Wejberg, H., Kareksela, S., Tzemi, D., Aro, L., Kuningas, S., Louhi, P., Ruuhijärvi, J., 2023. Euroopan unionin ennallistamisasetusehdotuksen luontotyyppi- ja turvemaatavoitteiden vaikutukset suomessa (no. 1/2023). Luonnonvara- ja biotalouden tutkimus.
Räsänen, A., Tolvanen, A., Kareksela, S., 2022. Monitoring peatland water table depth with optical and radar satellite imagery. Int. J. Appl. Earth Obs. Geoinformation 112, 102866. https://doi.org/10.1016/j.jag.2022.102866.
Räsänen, A., Virtanen, T., 2019. Data and resolution requirements in mapping vegetation in spatially heterogeneous landscapes. Remote Sens. Environ. 230, 111207. https://doi.org/10.1016/j.rse.2019.05.026.
Regulation (EU) 2024/1991, 2024. Regulation 2024/1991 of the European Parliament and of the Council on Nature Restoration and Amending Regulation (EU) 2022/869.
Riggs, R.M., Allen, G.H., David, C.H., Lin, P., Pan, M., Yang, X., Gleason, C., 2022. RODEO: an algorithm and google Earth engine application for river discharge retrieval from landsat. Environ. Model. Software 148, 105254. https://doi.org/10.1016/j.envsoft.2021.105254.
Rinne, J., Tuovinen, J.-P., Klemedtsson, L., Aurela, M., Holst, J., Lohila, A., Weslien, P., Vestin, P., Łakomiec, P., Peichl, M., Tuittila, E.-S., Heiskanen, L., Laurila, T., Li, X., Alekseychik, P., Mammarella, I., Ström, L., Crill, P., Nilsson, M.B., 2020. Effect of the 2018 European drought on methane and carbon dioxide exchange of northern mire ecosystems. Philos. Trans. R. Soc. B Biol. Sci. 375, 20190517. https://doi.org/10.1098/rstb.2019.0517.
Sadeghi, M., Babaeian, E., Tuller, M., Jones, S.B., 2017. The optical trapezoid model: a novel approach to remote sensing of soil moisture applied to Sentinel-2 and Landsat-8 observations. Remote Sens. Environ. 198, 52–68. https://doi.org/10.1016/j.rse.2017.05.041.

Sadeghi, M., Jones, S.B., Philpot, W.D., 2015. A linear physically-based model for remote sensing of soil moisture using short wave infrared bands. Remote Sens. Environ. 164, 66–76. https://doi.org/10.1016/j.rse.2015.04.007.
Sadeghi, M., Mohamadzadeh, N., Liang, L., Bandara, U., Caldas, M.M., Hatch, T., 2023. A new variant of the optical trapezoid model (OPTRAM) for remote sensing of soil moisture and water bodies. Sci. Remote Sens. 8, 100105. https://doi.org/10.1016/j.srs.2023.100105.
Sallinen, A., Akanegbu, J., Marttila, H., Tahvanainen, T., 2023. Recent and future hydrological trends of aapa mires across the boreal climate gradient. J. Hydrol. 617, 129022. https://doi.org/10.1016/j.jhydrol.2022.129022.
Sallinen, A., Tuominen, S., Kumpula, T., Tahvanainen, T., 2019. Undrained peatland areas disturbed by surrounding drainage: a large scale GIS analysis in Finland with a special focus on aapa mires. Mires Peat 1–22. https://doi.org/10.19189/MaP.2018.AJB.391.
Sass, G.Z., Creed, I.F., 2008. Characterizing hydrodynamics on boreal landscapes using archived synthetic aperture radar imagery. Hydrol. Process. 22, 1687–1699. https://doi.org/10.1002/hyp.6736.
Schultz, S., Millard, K., Darling, S., Chénier, R., 2023. Investigating the use of Sentinel-1 for improved mapping of small peatland water bodies: towards wildfire susceptibility monitoring in canada's boreal forest. Hydrology 10, 102. https://doi.org/10.3390/hydrology10050102.
Šimanauskienė, R., Linkevičienė, R., Bartold, M., Dąbrowska-Zielińska, K., Slavinskienė, G., Veteikis, D., Taminskas, J., 2019. Peatland degradation: the relationship between raised bog hydrology and normalized difference vegetation index. Ecohydrology 12. https://doi.org/10.1002/eco.2159.
Similä, M., Aapala, K., Penttinen, J. (Eds.), 2014. Ecological Restoration in Drained Peatlands – Best Practices from Finland. Metsähallitus, Vantaa.
Steenvoorden, J., Limpens, J., 2023. Upscaling peatland mapping with drone-derived imagery: impact of spatial resolution and vegetation characteristics. GIScience Remote Sens. 60, 2267851. https://doi.org/10.1080/15481603.2023.2267851.
Suding, K.N., 2011. Toward an era of restoration in ecology: successes, failures, and opportunities ahead. Annu. Rev. Ecol. Evol. Syst. 42, 465–487. https://doi.org/10.1146/annurev-ecolsys-102710-145115.
Tahvanainen, T., 2011. Abrupt ombrotrophication of a boreal aapa mire triggered by hydrological disturbance in the catchment: ombrotrophication of aapa mires. J. Ecol. https://doi.org/10.1111/j.1365-2745.2010.01778.x no-no.
Tucker, C.J., 1979. Red and photographic infrared linear combinations for monitoring vegetation. Remote Sens. Environ. 8, 127–150. https://doi.org/10.1016/0034-4257(79)90013-0.
Vasander, H., Tuittila, E.-S., Lode, E., Lundin, L., Ilomets, M., Sallantaus, T., Heikkilä, R., Pitkänen, M.-L., Laine, J., 2003. Status and restoration of peatlands in northern Europe. Wetl. Ecol. Manag. 11, 51–63. https://doi.org/10.1023/A:1022061622602.
Villoslada, M., Ylänne, H., Juutinen, S., Kolari, T.H.M., Korpelainen, P., Tahvanainen, T., Wolff, F., Kumpula, T., 2023. Reindeer control over shrubification in subarctic wetlands: spatial analysis based on unoccupied aerial vehicle imagery. Remote Sens. Ecol. Conserv, rse2.337. https://doi.org/10.1002/rse2.337.
Vogelmann, J.E., Rock, B.N., 1986. Assessing forest decline in coniferous forests of Vermont using NS-001 Thematic mapper simulator data. Int. J. Rem. Sens. 7, 1303–1321. https://doi.org/10.1080/01431168608948932.
Wickham, H., 2016. ggplot2, Use R! Springer International Publishing, Cham. https://doi.org/10.1007/978-3-319-24277-4.
Xu, H., 2006. Modification of normalised difference water index (NDWI) to enhance open water features in remotely sensed imagery. Int. J. Rem. Sens. 27, 3025–3033. https://doi.org/10.1080/01431160600589179.
Yu, Z., Loisel, J., Brosseau, D.P., Beilman, D.W., Hunt, S.J., 2010. Global peatland dynamics since the last glacial maximum. Geophys. Res. Lett. 37, 2010GL043584. https://doi.org/10.1029/2010GL043584.
Zhang, H.K., Roy, D.P., Yan, L., Li, Z., Huang, H., Vermote, E., Skakun, S., Roger, J.-C., 2018. Characterization of Sentinel-2A and Landsat-8 top of atmosphere, surface, and nadir BRDF adjusted reflectance and NDVI differences. Remote Sens. Environ. 215, 482–494. https://doi.org/10.1016/j.rse.2018.04.031.